HHS Public Access

Author manuscript

Audit Neurosci. Author manuscript; available in PMC 2021 January 27.

Published in final edited form as:

Audit Neurosci. 1996 ; 2: 241–255.

Autoradiographic Distribution of Muscarinic Acetylcholine Receptor Subtypes in Rat Cochlear Nucleus

WEIPING YAO,

DONALD A. GODFREY

Department of Otolaryngology, Head and Neck Surgery, Medical College of Ohio

Abstract

The cochlear nucleus (CN) receives cholinergic inputs primarily from centrifugal pathways. There is evidence that the effects of these cholinergic inputs may be mediated mainly by muscarinic acetylcholine receptors. We used 1-[N-methyl-^{3}H]scopolamine (NMS) to study muscarinic receptor binding in the rat CN autoradiographically. To determine which muscarinic receptor subtypes participate in the binding, we included competition assays using the unlabeled subtype-preferential ligands pirenzepine, AF-DX 116, 4-DAMP, HHSiD, and tropicamide to compete with [^{3}H]NMS for binding. Our results suggest that NMS binding density in the CN is about a tenth of that in the facial nucleus. Inside the CN, the highest binding was found in granular regions, followed in order by the dorsal CN (DCN) fusiform soma layer, the DCN molecular layer, the DCN deep layer, the anteroventral CN (AVCN) and posteroventral CN (PVCN). Binding in the interstitial nucleus (auditory nerve root) was similar to background. The results of the competition assays suggest that the M_2 receptor subtype predominates in VCN, M_4 in the DCN fusiform soma layer, and both subtypes in DCN molecular and deep layers. M_4 and M_3 subtypes predominated in the granular region of AVCN, while M_1 and M_2 were more prominent in the granular region of PVCN. The results show similarities to those obtained with pharmacological and immunohistochemical methods, but also some discrepancies. The different distributions of the different muscarinic receptor subtypes suggest that the effects of cholinergic inputs may differ among CN subregions, in agreement with *in vivo* pharmacological results. Overall, the centrifugal cholinergic influences on information processing in the CN may especially involve M_2 and M_4 receptors.

Keywords

4-DAMP; AF-DX 116; auditory; cholinergic; scopolamine; tropicamide

IT HAS BEEN KNOWN for some time that cholinergic synapses, deriving predominantly from more central locations, have an important role in the cochlear nucleus (CN) (Comis and Davies, 1969; Pickles and Comis, 1973; Godfrey et al., 1985, 1987). Although both nicotinic (Morley et al., 1977; Clarke *et al.*, 1985; Vetter and Heinemann, 1995) and muscarinic (Pickles and Comis, 1973; Wamsley et al., 1981; Yao and Godfrey, 1995; Chen

Correspondence: Weiping Yao, Department of Otolaryngology, Head and Neck Surgery, Medical College of Ohio, P.O. Box 10008, Toledo, OH 43699-0008.

et al., 1995) cholinergic receptors have been implicated in this function, recent evidence suggests that, in the dorsal CN (DCN), muscarinic receptors are much more prevalent (Chen *et al.*, 1994).

Muscarinic receptors in the CN have previously been localized using immunohistochemistry (Yao and Godfrey, 1995) as well as receptor binding with quinuclidinyl benzilate (QNB) (Wamsley et al., 1981; Whipple and Drescher, 1984; Frostholm and Rotter, 1986; Glendenning and Baker, 1988).

More recently, multiple subtypes of muscarinic receptors have been identified, both by pharmacological (subtypes M_1 – M_4) and molecular cloning (subtypes m1 – m5) methods. Further, there is evidence that different muscarinic receptor subtypes may have different specific functions (Hulme et al., 1990). So far there is little information about which of these subtypes are especially prevalent in the CN and where they are localized within it. It has been reported that m2 is the most abundant subtype in the brainstem, based on detection of proteins (Levey et al., 1991), mRNA (Buckley et al., 1988), and antagonist binding (Waelbroeck et al., 1986). A pharmacological study in slices found evidence for preferential involvement of muscarinic receptor subtypes M_2 and M_4 on neurons of the DCN (Chen et al., 1995). Further, immunohistochemistry with an antibody to the m2 subtype suggested its presence throughout most of the CN (Yao et al., 1995).

Based on the results noted above, we hypothesized that there should be different distribution patterns of the different muscarinic receptor subtypes, with M_2 and M_4 the most prominent, at least in the DCN. To test these hypotheses, we carried out autoradiography for muscarinic receptor binding, using 1-[N-methyl-^{3}H]scopolamine (NMS, a non-selective muscarinic antagonist), to map the distribution of muscarinic receptor binding in rat CN. The lower affinity of NMS, as compared to the previously used QNB, facilitates competitive binding studies. We then used several unlabeled subtype-preferential antagonists—pirenzepine(M_1, Hammer et al., 1980), AF-DX 116 (M_2, Giachetti et al., 1986), 4-DAMP (M_3, Waelbroeck et al., 1987), HHSiD (M_3, Lambrecht et al., 1989), and tropicamide (M_4, Lazareno et al., 1990) —to perform competitive binding to estimate quantitative distributions of M_1–M_4 subtypes among the rat CN subregions.

MATERIALS AND METHODS

Materials

1-[N-methyl-^{3}H]scopolamine ([^{3}H]NMS, 85 Ci/mmol), [^{3}H] Hyperfilm and Hypercassettes were from Amersham Life Science Corp. (Arlington Heights, IL). Atropine, pirenzepine (PZ) and tropicamide were from Sigma. Hexahydro-sila-difenidol (HHSiD) and 4-diphenylacetoxy-N-methylpiperidine methiodide (4-DAMP) were from RBI. 11[[2-[(diethylamino)methyl]-1-piperidinyl]acetyl]-5, 11-dihydro-6H-pyrido[2,3-b][1,4] benzodiazepine-6-one (AF-DX 116) was a gift from Boehringer Ingelheim, Inc. Emulsion NTB-2, developer D19 and Rapid Fixer were from Eastman Kodak. Other chemicals were obtained from either Sigma or Fisher.

Autoradiographic Receptor Binding

The radioactive ligand binding and autoradiography procedure was adapted from previous publications (Wamsley et al., 1980; Cortés and Palacios, 1986).

Tissue preparation: Young adult male Sprague-Dawley albino rats (200–300 g) were sacrificed by decapitation under sodium pentobarbital anesthesia (50 mg/kg, IP). Brain blocks were quickly removed and frozen on dry ice. Transverse sections 15 μm thick were cut through the cochlear nucleus (lower brainstem) using a microtome-cryostat (Hacker-Bright Instruments, Inc.) and thaw-mounted on gelatin-coated glass slides in alternating series. In some series, sections were mounted on gelatin-coated small glass coverslips so that they could be easily and accurately wiped off for post-binding scintillation counting. Sections on slides were vacuum-dried at room temperature for 2 hours and stored at −80°C (no longer than 3 days) until used.

Radioligand binding: Slide-mounted sections were brought to room temperature, washed with 0.1 M phosphate-buffered saline (PBS, pH 7.4) for 10 minutes, then incubated with [^{3}H]NMS in PBS for 60 minutes at room temperature, followed by two 5-minute washes with PBS at +4°C. In some initial experiments, sections were wiped from the slides with Whatman GF/C filters for liquid scintillation spectrometry to determine binding kinetics. Otherwise, slides were rinsed with +4°C deionized distilled water and then blow-dried and desiccated for 2 hours before proceeding with autoradiography. Binding equilibrium was tested over a range of 5 to 90 minutes incubation with 10 nM [^{3}H]NMS and was reached within 30 minutes, as determined by liquid scintillation counting of wiped sections. Saturable binding in the lower brainstem was determined by incubation with [^{3}H]NMS ranging from 0.1 nM to 20 nM. Nonspecific binding was determined in the presence of 1000 times concentration of atropine (e.g., 1 μM atropine with 1 nM [^{3}H]NMS) for each experiment.

Competition for muscarinic binding sites was assayed by incubating slide-mounted sections with 1 nM [^{3}H]NMS in the presence of various concentrations of subtype-preferential unlabeled ligands, including PZ (1–1000 nM), AF-DX 116 (0.1–10,000 nM), 4-DAMP (0.1–1000 nM), HHSiD (1–1000 nM) and tropicamide (0.1–1000 nM). As a control for nonspecific binding, incubation was done in the presence of 1 μM atropine in all the experiments.

Autoradiography: Autoradiograms were generated by apposing slide-mounted sections to [^{3}H]-sensitive Hyperfilm in a Hypercassette for two weeks at +4°C, followed by processing with Kodak developer D19 and fixing with Rapid Fixer. After exposure to the Hyperfilm, slides were dipped in NTB-2 emulsion (43°C), dried, and put in light-proof slide boxes with Drierite for another two weeks at 4°C before being developed, fixed, rinsed and air-dried. The sections were finally stained with cresyl violet to provide a cytoarchitectonic reference.

For quantitative calibration, a standard slide was included with each film. To generate the standard slides, tissue blocks consisting of rat brain homogenate mixed with serial concentrations of [^{3}H] NMS were prepared. Sections 15 μm thick were cut from these

blocks and collected either for scintillation counting to determine the radioactivity, for Lowry assay to determine the protein content, or for mounting on coated slides.

Microdensitometry

Computerized images of developed autoradiograms were taken and stored using NIH Image 1.44 (courtesy of Dr. E.I. Tietz, Department of Pharmacology, Medical College of Ohio). On these microimages, CN subregions were either identifiable or identified by staining with cresyl violet: anteroventral cochlear nucleus (AVCN), posteroventral cochlear nucleus (PVCN), dorsal cochlear nucleus deep layer (DCN-d), fusiform soma layer (DCN-f), and molecular layer (DCN-m), interstitial nucleus (IN, including auditory nerve root), and granular regions next to AVCN (Gr-A) and PVCN (Gr-P). Microdensitometric values of binding in these subregions and in the facial nucleus were obtained, corrected by subtracting the atropine control, and converted to radioactivity and ligand concentrations using the standard slide as a reference. Measurements for AVCN and Gr-A were made at middle-to-caudal locations.

Data Analysis

The features of [^{3}H]NMS binding to the CN regions—dissociation constant (K_d), maximum binding (B_{max}), and Hill coefficient—were obtained from saturation plots, Rosenthall plots and Hill plots. For analysis of competitive binding, the percentage inhibition of [^{3}H]NMS binding in each CN subregion was plotted vs. concentration for each ligand. From each competition curve, the IC50 (concentration of ligand that inhibits 50% of NMS binding) was obtained, and the competing ligand affinities (K_i) were estimated by the Cheng and Prusoff equation (Cheng and Prusoff, 1973), using the results of saturation binding of [^{3}H]NMS for each CN subregion.

Animals

The care and use of the animals reported on in this study were approved by the National Institutes of Health (NIDCD grant DC 00172-‘Microchemistry of the Cochlear Nucleus’) and by the Medical College of Ohio Institutional Animal Care and Use Committee.

RESULTS

Distribution of Muscarinic Receptor Binding Sites in the CN

At the level of the lower brainstem (Fig. 1), the facial nucleus (FN) contained a high density of muscarinic receptors (Wamsley et al., 1981; Cortés and Palacios, 1986) and therefore was used as a positive reference for our cochlear nucleus (CN) results. Our average value for the muscarinic receptor density in the FN (B_{max} = 1463 fmol/mg of protein) was similar to that in the literature (Cortés and Palacios, 1986). By comparison, the muscarinic receptor density ([^{3}H]NMS binding) in the CN was lower (5–25% of the FN in most regions) and showed subregional differences (Fig. 1).

Based on autoradiographic saturation analyses (Fig. 2), the quantitative distribution of muscarinic receptor binding among CN subregions was estimated (Table I). The most abundant [^{3}H]NMS binding was found in the granular regions next to both AVCN and

PVCN (Fig. 1a,c., Table I), while [^{3}H]NMS binding in the central portions of AVCN and PVCN was only 20–30% as much. [^{3}H]NMS binding in DCN was more abundant than in VCN and showed differences among layers: DCN-f > DCN-m > DCN-d (Fig. 1c., Table I). [^{3}H]NMS binding in the IN was almost undetectable (Fig. 1c) and not statistically different from background (not shown in Table I). The centrifugal labyrinthine bundle, which includes the OCB, appeared to be at least partially labeled with [^{3}H]NMS, but not in all sections (Fig. 1a,b). No [^{3}H]NMS binding was seen in the facial nerve root (FR, Fig. 1a).

In Gr-A, PVCN, and DCN-d, Hill coefficients were relatively low (Table I), suggesting that NMS binding to these CN subregions might involve negative cooperativity or more than one binding site.

Regional Distributions of Subtype-Preferential Muscarinic Antagonist Binding in the CN

The distributions of muscarinic receptor subtypes in the CN were examined by using unlabeled subtype-preferential antagonists to compete for [^{3}H]NMS binding sites (Fig. 3). The competition curves showed that the inhibitions of [^{3}H]NMS binding by the antagonists were dose-dependent (Fig. 4). The inhibition parameters (IC_{50} and K_i) of these antagonists are summarized in Table II.

In AVCN and PVCN, the inhibitions of [^{3}H]NMS by PZ, 4-DAMP, HHSiD and tropicamide were less than 50% at all ligand concentrations tested (Fig. 4); therefore, no IC_{50} and K_i values were obtained (Table II). Among CN subregions, all tested ligands showed a range of binding affinities, but AF-DX 116 showed an especially wide range (Table II). This heterogeneous binding profile may be a reflection of the variety of Hill coefficients and K_d values for NMS binding in the CN, suggesting the presence of multiple receptor subtypes and /or binding sites, in contrast to the FN, where it appears that only one subtype (M_2) predominates (Buckley et al., 1988; Levey et al., 1991; Vilario et al., 1992; Table II). To assess potential involvement of muscarinic receptor subtypes, the binding affinities for the ligands were compared with values averaged from the literature, particularly for cloned receptor subtypes (Table III). All the ligands can bind to all muscarinic receptor subtypes, but each has a highest affinity (lowest K_i) for its preferred subtype (i.e., PZ for M_1, AF-DX 116 for M_2, 4-DAMP and HHSiD for M_3, and tropicamide for M_4). We divided the K_i values for different CN regions into a high-affinity group, likely to be binding particularly to the preferred subtype for the ligand, and a low-affinity group (Table II). The cutoff value chosen for division into these two groups was the mean plus one standard deviation of the literature values for each ligand with its preferred subtype. Since only one source of K_i for tropicamide could be found, the standard deviations were arbitrarily set equal to the averages of those for the other ligands. High affinity binding of tropicamide (M_4 preference) was found in all CN regions except AVCN and PVCN, while that of AF-DX 116 (M_2 preference) was found in all regions except Gr-A. By comparison, high-affinity binding of the ligands with preferences for M_1 and M_3 subtypes were found in fewer regions.

The amount of each receptor subtype in each CN region was estimated by measuring, from. Figure 4, the percentage reduction of [^{3}H]NMS binding at a concentration of competing ligand equal to the average of the high-affinity K_is for that ligand in the CN (Table II).

Multiplication of these percentage reductions by the total [^{3}H]NMS binding for each region provided a rough estimate of the amount of each subtype in each region (Fig. 5).

Based on these estimates, only the M_2 receptor subtype appeared to be prominent in the central portions of AVCN and PVCN.

The granular regions of AVCN (Gr-A) and PVCN (Gr-P) had different results for prevalence of muscarinic receptor subtypes. In Gr-A, subtypes M_3 and M_4 were more prominent than M_1 or M_2 (although the K_i values for HHSiD and 4-DAMP were somewhat high). On the other hand, Gr-P had a surprisingly high prevalence of M_1, as well as some representation of all other subtypes.

Except in the DCN deep and molecular layers, the binding of 4-DAMP and HHSiD gave comparable estimates for the prevalence of M_3 receptors (Fig. 5). In making conclusions about M_3 receptors, we gave preference to the results with HHSiD because of its higher selectivity for M_3 relative to M_2 or M_5 (Table III).

In all layers of the DCN, M_4 receptors were especially prominent, but M_2 receptors were also prominent, particularly in the molecular layer.

Based on the competitive binding of the preferential antagonists across regions (Fig. 5), all known muscarinic receptor subtypes have some representation in the CN, although M_2 and M_4 are dominant. The estimated binding site concentrations for M_4 and M_3 were especially high in the superficial layers of the DCN and granular regions. M_2 sites were especially concentrated in the molecular layer of the DCN and the granular region next to PVCN, but were also well represented elsewhere in the CN. M_1 sites had a strikingly high concentration in the granular region next to PVCN.

Only AF-DX 116 demonstrated relatively high affinity binding in the facial nucleus, in agreement with previous evidence for predominance there of the M_2 receptor subtype (Spencer et al., 1986; Buckley et al., 1989; Levey et al., 1991,1995).

DISCUSSION

[^{3}H]NMS has previously been suggested to have similar affinities for all muscarinic receptor subtypes (Wamsley et al., 1980; Cortés and Palacios, 1986; Ehlert et al., 1989; Smith et al., 1990) and was used in the present study to demonstrate the whole population of muscarinic receptors in the CN. Our results for [^{3}H]NMS binding to the FN, which contained a high density of muscarinic receptors and was used as our positive reference, are similar to those in the literature (Wamsley et al., 1981; Cortés and Palacios, 1986). Concentrations of muscarinic receptors in the CN averaged about 11% of those in the FN. Most of the muscarinic receptors in the CN were concentrated in the regions where granule cell somata and terminals predominate: granular regions next to AVCN and PVCN and the fusiform soma and molecular layers of DCN.

Comparisons with [^{3}H]QNB Binding in the CN

The distribution pattern of [^{3}H]NMS binding was generally in agreement with that of [^{3}H]QNB binding in rat CN, which appeared to be related to the granular regions (Wamsley et al., 1981), and in mouse CN, in which [^{3}H]QNB binding sites were seen in the molecular layer, possibly extending into the pyramidal (i.e., fusiform soma) layer of DCN, and in the granular region next to PVCN (Frostholm and Rotter, 1986). In cat CN, [^{3}H]QNB binding was also closely associated with granule cells (Glendenning and Baker, 1988). Our higher values for [^{3}H]NMS binding in DCN than in VCN agree with a biochemical quantitation of [^{3}H]QNB binding in guinea pig CN (Whipple and Drescher, 1984). Thus, the localization of muscarinic receptor binding in the CN is consistent across different ligands and different species.

Comparisons with Immunolocalization of Muscarinic Receptor Proteins

There are discrepancies between our [^{3}H]NMS binding results and our previous immunohistochemical results for distribution of muscarinic receptor proteins in rat CN (Yao and Godfrey, 1995). With M35, an anti-muscarinic-receptor antibody, muscarinic receptor proteins were, unlike [^{3}H]NMS and [^{3}H]QNB binding, mostly found in VCN, less in DCN, and even less in granular regions. Further, M35 labeling in the DCN fusiform soma layer, where there is a high density of granule cells, was not associated with the granule cells, but with larger cells (Yao and Godfrey, 1995). There are some possible explanations for these discrepancies. For immunolocalization of mAChR, the specificity and positive/negative controls (André et al., 1983, 1984; Van der Zee et al., 1989; Yao and Godfrey, 1995) should have been able to exclude false-positive immunolabeling. A more likely false-negative in M35 labeling might have resulted from failure of penetration of the antibody to small cells or fibers and terminals, especially in and near the granular regions. Our previous suggestion that M35 may not detect m2 receptors (Yao and Godfrey, 1995) even worsens the discrepancy in magnocellular VCN, because most of the muscarinic receptor binding there appeared to be associated with M_2. For receptor binding, it is unlikely that our results included false positive [^{3}H]NMS binding in the CN, given the agreement with [^{3}H]QNB binding in CN (Wamsley et al., 1981) and other data in the literature (Cortés and Palacios, 1986; Ehlert et al., 1989; Hulme et al., 1990), and given the atropine specificity control. However, there are some possible explanations for the low [^{3}H]NMS binding in magnocellular VCN: (1) Tritium quenching may result in underestimates of [^{3}H]NMS binding in the white-matter-rich IN, magnocellular VCN, and DCN deep layer. This is a potential problem for autoradiography using tritiated ligands. The magnitude of absorption is dependent upon the density of the tissue (dry mass per unit volume) (Kuhar and Unnerstall, 1985; Kuhar, 1986). Previous measurements indicate that IN, AVCN, PVCN, and the deep layer of DCN have higher dry weights per volume than granular regions and the molecular and fusiform soma layers of DCN (Godfrey et al., 1978). (2) M35-revealed muscarinic receptor proteins in the magnocellular VCN, although functionally important, may have low binding affinity for [^{3}H]NMS (Herkenham and McLean, 1986). (3) M35-labeled muscarinic receptors may include some unidentified subtype(s) with low affinity for [^{3}H]NMS. (4) Large cells of magnocellular VCN might be muscarinic-cholinoceptive, but have immunoreactivity for M35 mostly concentrated in their somata, while binding sites for muscarinic ligands might be mostly on their dendrites. Such an explanation could fit

with the model of Benson and Brown (1990) for OCB innervation of CN neurons, wherein fibers terminate in or near granular regions, but on the dendrites of neurons with somata in magnocellular VCN.

Comparisons with AChE and ChAT

The distribution of muscarinic receptor binding sites in rat CN is highly correlated with that of histochemical staining for AChE activity ($r = 0.86$, $P < 0.05$), which is closely associated with granular regions in the CN (Osen et al., 1984; Yao and Godfrey, 1995). This would be consistent with colocalization of binding sites for acetylcholine with its degradative enzyme. On the other hand, [^{3}H]NMS binding sites and ChAT immunoreactivity differ from each other in their distributions, particularly in the relative distributions between magnocellular VCN and granular regions. Anatomical mismatch between the distributions of transmitters, or their synthetic enzymes, and receptor binding has been reported previously and suggested to possibly result from technical limitations or actions of transmitters at sites distant from where they are released (Herkenham, 1986, 1987; Spencer et al., 1986; Ernsberger et al., 1988).

Overall, the available evidence for localization of markers for cholinergic transmission indicates a dichotomy in the VCN: ChAT enzyme activity and ChAT-immunoreactive puncta, presumably representing cholinergic terminals, as well as M35 immunoreactivity, are particularly concentrated in VCN magnocellular regions, whereas [^{3}H]NMS and [^{3}H]QNB binding sites, as well as AChE activity, are especially prominent in granular regions. The resolution of this notable discrepancy requires further study. There is evidence for nicotinic acetylcholine receptors in the CN (Morley et al., 1977; Hunt and Schmidt, 1978; Swanson et al., 1987; Wada et al., 1989; Vetter and Heinemann, 1995), which may at least partially represent the cholinoceptive counterpart to the cholinergic innervation (ChAT-labeled puncta) in the CN regions (especially AVCN and PVCN) where muscarinic receptor binding was not prominent.

Subtype-Preferential Muscarinic Antagonist Binding in Rat CN

Pharmacological classification of receptor subtypes is based on the binding of subtype-selective antagonists. In the present study, prevalences of muscarinic receptor subtypes were estimated by inhibition of [^{3}H]NMS binding with unlabeled antagonists. The results of our autoradiographic competition assays suggested a complex muscarinic receptor subtype profile in rat CN. However, the low selectivities of the antagonists, wherein none exhibits much greater affinity for one subtype over all others (Hulme et al., 1990; Table III), complicated the analysis of these results and led us to refer to the antagonists as subtype-preferential rather than subtype-selective. In some CN regions, competitive binding curves, especially for AF-DX 116, could be more closely fit with a two-binding-site model, including both high- and low-affinity binding sites. However, this more sophisticated approach to analysis of the binding did not seem clearly justified for antagonists with relatively low selectivity and has not provided consistent results in the past (Hulme et al., 1990). Therefore, our analysis of competitive binding results was based on a simpler one-binding-site model.

Our high-affinity K_is for the antagonists were generally comparable to the literature values, except for some extremely low AF-DX 116 values in AVCN and PVCN. It is possible that these very low K_i values represent errors related to the relatively low density of [^{3}H]NMS binding and the low Hill coefficients in AVCN and PVCN. However, there is other evidence that AF-DX 116 may show a relatively wide range of affinities over different muscarinic receptor subtypes (Batink et al., 1987; Hulme et al., 1990). Also, there is evidence that AF-DX 116 recognizes some very high affinity binding sites in the brainstem (Messer et al., 1992). The extremely high affinities of AF-DX 116 in AVCN and PVCN might correlate with the few neurons immunoreactive to m2-specific antibody (Yao et al., 1995). On the basis of our criteria, only AF-DX 116 demonstrated a high-affinity K_i in the facial nucleus, in agreement with other evidence that almost all muscarinic receptors in the facial nucleus are of the M_2 subtype (Spencer et al., 1986; Buckley et al., 1989; Levey et al., 1991, 1995).

Overall, M_2 and M_4 appear to be the most prevalent muscarinic receptor subtypes in tire CN. The results are generally in agreement with results of m2 immunohistochemistry (Yao et al., 1995) and the results of electrophysiological studies on the DCN (Chen et al., 1995). Both m2 immunoreactivity and high-affinity binding for AF-DX 116 were found in all CN subregions. In granular regions of AVCN and PVCN and their vicinity, [^{3}H]NMS binding and m2 immunolabeling were somewhat different. Examined with the cresyl violet-stained sections, [^{3}H]NMS did not reveal preferential binding to a subgranular layer, which was prominently labeled in the m2 immunohistochemistry. Preferential binding of AF-DX 116 to a subgranular layer also could not be shown. In DCN, AF-DX 116 binding appeared more prevalent in the molecular layer than in the deep and fusiform soma layers, while m2 immunoreactivity had similar staining densities across the three layers. One possible explanation for the discrepancies between AF-DX 116 binding and m2 immunoreactivity in the granular regions and DCN might be the presence of an axonally transported form of the receptor, visible with m2 immunolabeling, but less accessible to [^{3}H]NMS or having a lower binding affinity. This explanation would agree with the apparently inconsistent [^{3}H]NMS binding to the fiber bundle containing the OCB.

Functional Considerations

The evidence for muscarinic receptor binding sites in the CN is complementary to the evidence that there is a cholinergic input to the CN and is consistent with the evidence that cholinergic effects on DCN neurons are primarily mediated by muscarinic receptors (Chen et al., 1994a, 1995). The presence of multiple subtypes of muscarinic receptors suggests heterogeneity of muscarinic receptor functions in the CN. Through different subtypes of muscarinic receptors, the effects of the same neurotransmitter, acetylcholine, could vary among different CN subregions or upon different neurons within a subregion. This may be consistent with *in vivo* pharmacological results (Caspary et al., 1983).

The predominance of M_4 receptors in the DCN is consistent with evidence for M_4 receptor influences on both regular and bursting neurons in slices of DCN (Chen et al., 1995). Further, our evidence for particularly high concentrations of M_4 receptors in the fusiform soma layer agrees with the predominant localization there of recordings from regular and bursting neurons (Waller arid Godfrey, 1994; Chen et al., 1994a, 1995). Many of the regular

neurons in. these slices should represent the activity of DCN fusiform cells, while most of the bursting neurons should represent the activity of cartwheel cells (Manis et al., 1993; Zhang and Oertel, 1993; Waller and Godfrey, 1994). Evidence has also been reported that muscarinic effects on bursting neurons may be indirect, through activation of granule cells, and that M_2 as well as M_4 receptors are probably involved (Chen et al., 1994a, 1995). The evidence presented here for a higher concentration of M_2 receptors in the molecular layer than in the fusiform soma layer of DCN suggests that muscarinic receptors on granule cells may include the M_4 subtype especially near their somata in the fusiform soma layer and the M_2 subtype especially on the terminals of their parallel fibers in the molecular layer (Wouterlood and Mugnaini, 1984). Since the muscarinic effects in the DCN in slices appear to be entirely excitatory, the evidence from these two studies may suggest the presence of M_2 muscarinic receptors on parallel fiber terminals that promote release of neurotransmitter glutamate (Oliver et al., 1983; Manis et al., 1993; Chen et al., 1994b; Waller et al., 1994).

The possibility that the multiple subtypes of muscarinic receptors may be correlated to some extent with the multiple neuronal types in the CN showing muscarinic receptor immunoreactivity (Yao and Godfrey, 1995) will need to be studied by other methods, such as immunohistochemistry (Yao et al., 1995) or *in situ* hybridization (Yao et al., 1994). M_2 receptors, many of which have been suggested to be presynaptic autoreceptors (Potter et al., 1983; Spencer et al., 1986), were found to some extent in all CN regions except IN, consistent with the widespread presence of cholinergic terminals throughout the rat CN (Godfrey, 1993; Vetter et al., 1993; Yao and Godfrey, 1995).

Overall, muscarinic receptors in the CN have been found to have effects on detection of acoustic signals in a noisy background (Pickles and Comis, 1973; Pickles, 1988). How this results from the functions of the individual subtypes, and whether there are other particular functions of the subtypes as suggested by their different localizations, will need to be the subjects of future behavioral studies.

ACKNOWLEDGMENTS

We are grateful to Dr. E.I. Tietz, Department of Pharmacology, Medical College of Ohio, for her generous advice and provision of resources for the quantitative measurement of autoradiographic densities. We also thank Dr. W.S. Messer, Jr., University of Toledo, and Dr. T. Chiu, Department of Pharmacology, Medical College of Ohio, for advice (although not always followed) on analysis of muscarinic receptor binding data. This study was supported by Grant DC 00172 from the National Institute of Deafness and other Communication Disorders, NIH.

Table of Abbreviations

4-DAMP	4-diphenylacetoxy-N-methylpiperidine methiodide
AChE	acetylcholinesterase
AChR	acetylcholine receptor
AVCN	anteroventral cochlear nucleus
AF-DX 116	11[[2-[(diethylamino)methyl]-1-piperidinyl]acetyl]-5,11-dihydro-6H-pyrido[2,3-b][1,4] benzodiazepine-6-one

B_{max}	maximum binding
Cb	cerebellum
ChAT	choline acetyltransferase
CN	cochlear nucleus
DCN	dorsal cochlear nucleus
DCN-d	dorsal cochlear nucleus deep layer
DCN-f	dorsal cochlear nucleus fusiform soma layer
DCN-m	dorsal cochlear nucleus molecular layer
FN	facial nucleus
FR	facial motor nerve root
Gr-A	granular regions lateral to anteroventral cochlear nucleus
Gr-P	granular regions lateral to posteroventral cochlear nucleus
HHSiD	hexahydro-sila-difenidol
IN	interstitial nucleus, including auditory nerve root
K_d	dissociation constant
mAChR	muscarinic acetylcholine receptor
NMS	N-methyl-scopolamine
OCB	olivocochlear bundle
PVCN	posteroventral cochlear nucleus
PZ	pirenzepine
QNB	quinuclidinyl benzilate
STT	spinal trigeminal tract
TB	trapezoid body
VR	vestibular nerve root

REFERENCES

André C, De Packer JP, Vanderheyden P, Vauquelin G and Strosberg AD (1983). Purification of muscarinic acetylcholine receptors by affinity chromatography. EMBO J. 2, 499–504. [PubMed: 6605245]

André C, Guillet JG, De Packer JP, Vanderheyden P, Hoebeke J and Strosberg AD (1984). Monoclonal antibodies against the native or denatured forms of muscarinic acetylcholine receptors. EMBO J. 3, 17–21. [PubMed: 6200320]

Batink HD, Davidesko D, Doods HN, van Charldorp KJ, de Jonge A and van Zwieten PA (1987). Subdivision of M_2-receptors into three types. Br. J. Pharmacol 90, 81P. [PubMed: 2434180]

Bonner TI (1989). The molecular basis of muscarinic receptor diversity. TINS, 12(4), 148–151. [PubMed: 2470172]

Buckley NJ, Bonner TI and Brann MR (1988). Localization of a family of muscarinic receptors in rat brain. J. Neurosci 8, 4646–4652. [PubMed: 3199198]

Buckley NJ, Bonner TI, Buckley CM and Brann MR (1989). Antagonist binding properties of five cloned muscarinic receptors expressed in CHO-K1 cells. Mol. Pharmacol 35, 469–476. [PubMed: 2704370]

Caspary DM, Havey DC and Faringold CL (1983). Effects of acetylcholine on cochlear nucleus neurons. Exp. Neurol 82, 491–498. [PubMed: 6628633]

Chen K, Waller HJ and Godfrey DA (1994a). Cholinergic modulation of spontaneous activity in rat dorsal cochlear nucleus. Hearing Res. 77, 168–176.

Chen K, Waller HJ and Godfrey DA (1994b). Glutamate antagonists affect cholinergic activation of bursting neurons in rat dorsal cochlear nucleus. Abstr. Assoc. Res. Otolaryngol 17, 13.

Chen K, Waller HJ and Godfrey DA (1995). Muscarinic receptor subtypes in rat dorsal cochlear nucleus. Hearing Res. 89, 137–145.

Cheng Y and Prusoff WH (1973). Relationship between the inhibition constant (K_1) and the concentration of inhibitor which causes 50 per cent inhibition (IC_{50}) of an enzymatic reaction. Biochemical Pharmacology, 22, 3099–3108. [PubMed: 4202581]

Cortés R and Palacios JM (1986). Muscarinic cholinergic receptor subtypes in the rat brain. I. Quantitative autoradiographic studies. Brain Res. 362, 227–238. [PubMed: 3942874]

Dörje F, Wess J, Lambrecht F, Tacke R, Mustschler E and Brann MR (1991). Antagonist binding profiles of five cloned human muscarinic receptor subtypes. J. Pharmacol. Exp. Ther 256, 727–733. [PubMed: 1994002]

Ehlert FJ, Delen FM, Yun SH, Friedman DJ and Self DW (1989). Coupling of subtypes of the muscarinic receptor to adenylate cyclase in the corpus striatum and heart. J. Pharm. Exp. Ther 251, 660–671.

Ehlert FJ and Tran LP (1990). Regional distribution of M_1, M_2 and non-M_1, non-M_2 subtypes of muscarinic binding sites in rat brain. J. Pharm. Exp. Ther 255, 1148–1157.

Ernsberger P, Arneric SP, Arango V and Reis DJ (1988). Quantitative distribution of muscarinic receptors and choline acetyltransferase in rat medulla: examination of transmitter-receptor mismatch. Brain Res. 452, 336–344. [PubMed: 3401740]

Fernando JC, Abdallah EA, Evinger M, Forray C and el-Fakahany EE (1991). The presence of an M_4 subtype muscarinic receptor in the bovine adrenal medulla revealed by mRNA and receptor binding analyses. Eur. J. Pharmacol 207, 297–303. [PubMed: 1723686]

Frey KA and Howland MM (1992). Quantitative autoradiography of muscarinic cholinergic receptor binding in the rat brain: distinction of receptor subtypes in antagonist competition assays. J. Pharm. Exp. Ther 263, 1391–1400.

Frostholm A and Rotter A (1986). Autoradiographic localization of receptors in the cochlear nucleus of the mouse. Brain Res. Bull 16, 189–203. [PubMed: 3008955]

Giachetti A, Micheletti R and Montagna E (1986). Cardioselective profile of AF-DX 116, a muscarine M_2 receptor antagonist. Life Sci. 38, 1663–1672. [PubMed: 3754611]

Glendenning KK and Baker BN (1988). Neuroanatomical distribution of receptors for three potential inhibitory neurotransmitters in the brainstem auditory nuclei of the cat. J. Comp. Neurol 275, 288–308. [PubMed: 2851616]

Godfrey DA (1993). Comparison of quantitative and immunohistochemistry for choline acetyltransferase in the rat cochlear nucleus. In: The Mammalian Cochlear Nuclei: Organization and Function, Merchan MA, Juiz JM, Godfrey DA, and Mugnaini E, eds., Plenum Publ. Corp., New York, pp 267–276.

Godfrey DA and Matschinsky FM (1981). Quantitative distribution of choline acetyltransferase and acetylcholinesterase activities in the rat cochlear nucleus. J. Histochem. Cytochem 29, 720–730. [PubMed: 7252132]

Godfrey DA, Carter JA, Lowry OH and Matschinsky FM (1978). Distribution of gamma-aminobutyric acid, glycine, glutamate and aspartate in the cochlear nucleus of the rat. J. Histochem. Cytochem 26, 118–126. [PubMed: 624832]

Godfrey DA, Park JL, Rabe JR, Dunn JD and Ross CD (1983). Effects of large brain stem lesions on the cholinergic system in the rat cochlear nucleus. Hearing Res. 11, 133–156.

Godfrey DA, Park JL, Dunn JD and Ross CD (1985). Cholinergic neurotransmission in the cochlear nucleus. In: Auditory Biochemistry, Drescher DG, ed., Thomas CC, Springfield, Illinois, pp 163–183.

Godfrey DA, Park-Hellendall JL, Dunn JD and Ross CD (1987). Effects of trapezoid body and superior olive lesions on choline acetyltransferase activity in the rat cochlear nucleus. Hearing Res. 28, 253–270.

Hammer R, Berrie CP, Birdsall NJM, Burgen ASV and Hulme EC (1980). Pirenzepine distinguishes between different subclasses of muscarinic receptors. Nature (Lond.). 283, 90–92. [PubMed: 7350532]

Henderson Z and Sherriff FE (1991). Distribution of choline acetyltransferase immunoreactive axons and terminals in the rat and ferret brainstem. J. Comp. Neurol 314, 147–163. [PubMed: 1797870]

Herkenham M (1987). Mismatches between neurotransmitter and receptor localizations in brain: observations and implications. Neuroscience. 23, 1–38. [PubMed: 2891080]

Herkenham M and McLean S (1986). Mismatches between receptor and transmitter localizations in the brain. In. Quantitative Receptor Autoradiography. Kuhar MJ, ed., Liss, New York, pp. 137–171.

Hulme EC, Birdsall NJM and Buckley NJ (1990). Muscarinic receptor subtypes. Ann. Rev. Pharmacol. Toxicol 30, 633–673. [PubMed: 2188581]

Hunt S and Schmidt J (1978). Some observations on the binding patterns of α-bungarotoxin in the central nervous system of the rat. Brain Res. 157, 213–232. [PubMed: 719523]

Kashihara K, Varga EV, Waite SL, Roseke WR and Yamamura HI (1992). Cloning of the rat M_3, M_4 and M_5 muscarinic acetylcholine receptor genes by the polymerase chain, reaction (PCR) and the pharmacological characterization of the expressed genes. Life Sci. 51, 955–971. [PubMed: 1325587]

Kuhar MJ (1986). Quantitative receptor autoradiography: an overview. In: Quantitative Receptor Autoradiography, Boast CA, Snowhill EW, and Altar CA, eds., Alan R. Liss, Inc., New York, pp. 1–12.

Kuhar MJ and Unnerstall JR (1985). Quantitative receptor mapping by autoradiography: some current technical problems. TIPS. 8, 49–53.

Lambrecht G, Feifel R, Wagner-Röder M, Strohmann C, Zilch H, Tacke R, Waelbroeck M, Christophe J, Boddeke H and Mutschler E (1989). Affinity profiles of hexahydro-sila-difenidol analogues at muscarinic receptor subtypes. Eur. J. Pharmacol 168, 71–80. [PubMed: 2583233]

Lazareno S, Buckley NJ and Roberts FF (1990). Characterization of muscarinic M_4 binding sites in rabbit lung, chicken heart, and NG108-15 cells. Mol. Pharmacol 38, 805–815. [PubMed: 2250662]

Lazareno S and Birdsall NJM (1993). Pharmacological characterization of acetylcholine-stimulated [^{35}S]-GTPrS binding mediated by human muscarinic receptors m1–m4: antagonist studies. Br. J. Pharmacol 109, 1120–1127. [PubMed: 8401923]

Levey AI, Kitt CA, Simonds WF, Price DL and Brann MR (1991). Identification and localization of muscarinic acetylcholine receptor proteins in brain with subtype-specific antibodies. J. Neurosci 11, 3218–3226. [PubMed: 1941081]

Levey AI, Edmunds SM, Hersch SM, Wiley RG and Heilman CJ (1995). Light and electron microscopic study of m2 muscarinic acetylcholine receptor in the basal forebrain of the rat. J. Comp. Neurol 351, 339–356. [PubMed: 7706546]

Manis PB, Scott CJ and Spirou GA (1993). Physiology of the dorsal cochlear nucleus molecular layer. In: The Mammalian Cochlear Nuclei: Organization and Function, Merchan MA, Juiz JM, Godfrey DA, and Mugnaini E, eds., Plenum Publ. Corp., New York, pp. 361–371.

Messer WS Jr., Ngur DO, Ellerbrock BR and Hoss W (1992). Novel muscarinic receptor binding and phosphoinositol response in the midbrain and brainstem. In: Recent Advances in Cellular and Molecular Biology: Neurobiochemical Transmitter Pathways, Adrenoceptors and Muscarinic Receptors. Wegmann RJ, and Wegmann MA, eds., Peeters Press, Leuven, Belgium, pp. 267–272.

Morley BJ, Lorden JF, Brown GB, Kemp GE and Bradley RJ (1977). Regional distribution of nicotinic acetylcholine receptor in rat brain. Brain Res. 134, 161–166. [PubMed: 912415]

Oertel D and Wu SH (1989). Morphology and physiology of cells in slice preparations of the dorsal cochlear nucleus of mice. J. Comp. Neurol 283, 228–247. [PubMed: 2738197]

Oliver DL, Potashner SJ, Jones DR and Morest DK (1983). Selective labeling of spiral ganglion and granule cells with D-aspartate in the auditory system of cat and guinea pig. J. Neurosci 3, 455–472. [PubMed: 6131111]

Osen KK, Mugnaini E, Dahl AL and Christiansen AH (1984). Histochemical localization of acetylcholinesterase in the cochlear and superior olivary nuclei: A reappraisal with emphasis on the cochlear granule cell system. Archives Italiennes de Biologie. 122, 169–212. [PubMed: 6517650]

Pickles JO (1988). An Introduction to the Physiology of Hearing. Academic Press, Inc., San Diego, California.

Pickles JO and Comis SD (1973). Role of centrifugal pathways to cochlear nucleus in detection of signals in noise. J. Neurophysiol 36, 1131–1137. [PubMed: 4761723]

Potter LT, Flynn DD, Hanchett HE, Kalinoski DL, Luber-Narod J and Mash DC (1983). Independent M_1 and M_2 receptors: ligands, autoradiography and functions. Trends Pharmacol. Sci, (Suppl.), 22–23.

Smith TD, Annis SJ, Ehlert FJ and Leslie FM (1990). N-[^{3}H]Methylscopolamine labeling of non-M1, Non-M2 muscarinic receptor binding sites in rat brain. J. Pharmacol. Exp. Ther 256, 1173–1181.

Spencer DG, Horvath E and Traber J (1986). Direct autoradiographic determination of M1 and M2 muscarinic acetylcholine receptor distribution in the rat brain: relation to cholinergic nuclei and projections. Brain Res. 380, 59–68. [PubMed: 3756473]

Swanson LW, Simmons DM, Whiting PJ and Lindstrom J (1987). Immunohistochemical localization of neuronal nicotinic receptors in the rodent central nervous system. J. Neurochem 7, 3334–3342.

Tago H, McGeer PL, McGeer EG, Akiyama H and Hersh LB (1989). Distribution of choline acetyltransferase immunopositive structures in the rat brainstem. Brain Res. 495, 271–297. [PubMed: 2765931]

Van der Zee EA, Matsuyama T, Strosberg AD, Traber J and Luiten PGM (1989). Demonstration of muscarinic acetylcholine receptor-like immunoreactivity in rat forebrain and upper brainstem. Histochemistry. 92, 475–485. [PubMed: 2807994]

Vetter DE, Cozzari C, Hartman BK and Mugnaini E (1993). Choline acetyltransferase in the rat cochlear nuclei: immunolocalization with a monoclonal antibody. In: The Mammalian Cochlear Nuclei: Organization and Function, Merchan MA, Juiz JM, Godfrey DA, and Mugnaini E, eds., Plenum Publ. Corp., New York, pp. 279–290.

Vetter DE and Heinemann SF (1995). Expression of nicotinic acetylcholine receptor subunits in the rat cochlear nucleus. Soc. Neurosci. Abstr 21, 402.

Vilario MT, Wiederhold KH, Palacios JM and Mengod G (1992). Muscarinic M_2-selective ligands also recognize M_4 receptors in the rat brain: evidence from combined in situ hybridization histochemistry and receptor autoradiography. Synapse. 11, 171–183. [PubMed: 1636148]

Wada E, Wada K, Boulter J, Deneris E, Heinemann S, Patrick J and Swanson LW (1989). Distribution of Alpha2, Alpha3, Alpha4, and Beta2 neuronal nicotinic receptor subunit mRNAs in the central nervous system; a hybridization histochemical study in the rat. J. Comp. Neurol 284, 314–835. [PubMed: 2754038]

Waelbroeck M, Gillard M, Robberecht P and Christophe J (1986). Kinetic studies of [^{3}H]-N-methylscopolamine binding to muscarinic receptors in the rat central nervous system: evidence for the existence of three classes of binding sites. Mol. Pharmacol 30, 305–314. [PubMed: 3762520]

Waelbroeck M, Camus J, Winand J and Christophe J (1987). Different antagonist binding properties of rat pancreatic and cardiac muscarinic receptors. Life Sci. 41, 2235–2240. [PubMed: 3118122]

Waller HJ and Godfrey DA (1994). Functional characteristics of spontaneously active neurons in rat dorsal cochlear nucleus in vitro. J. Neurophysiol 71, 467–478. [PubMed: 8176420]

Waller HJ, Godfrey DA and Chen K (1994). Responses of dorsal cochlear nucleus neurons to electrical stimulation of parallel fibers in rat brain stem slices. Abstr. Assoc. Res. Otolaryngol 17, 12.

Wamsley JK, Zarbin MA, Birdsall NJM and Kuhar MJ (1980). Muscarinic cholinergic receptors: autoradiographic localization of high and low affinity agonist binding sites. Brain Res. 200, 1–12. [PubMed: 7417800]

Wamsley JK, Lewis MS, Young WS and Kuhar MJ (1981). Autoradiographic localization of muscarinic cholinergic receptors in rat brainstem. J. Neurosci 1, 176–191. [PubMed: 7264716]

Whipple MR and Drescher DG (1984). Muscarinic receptors in the cochlear nucleus and auditory nerve of the guinea pig. J. Neurochem 43, 192–198. [PubMed: 6726247]

Wouterlood FG and Mugnaini E (1984). Cartwheel neurons of the dorsal cochlear nucleus: a Golgi-electron microscopic study in rat. J. Comp. Neurol 227, 136–157. [PubMed: 6088594]

Yao W, Godfrey DA and Budd GC (1994). Muscarinic acetylcholine receptors in rat cochlear nucleus: an in situ hybridization histochemistry study. Abstr. Assoc. Res. Otolaryngol 17, 12.

Yao W and Godfrey DA (1995). Immunohistochemistry of muscarinic receptors in rat cochlear nucleus. Hearing Res. 89, 76–85.

Yao W, Godfrey DA and Levey AI (1995). Immunolocalization of m2 muscarinic acetylcholine receptors in rat cochlear nucleus. Soc. Neurosci. Abstr 25, 403.

Zhang S and Oertel D (1993). Cartwheel and superficial stellate cells of the dorsal cochlear nucleus of mice: intracellular recordings in slices. J. Neurophysiol 69, 1384–1397. [PubMed: 8389821]

Zubieta JK and Frey DA (1993). Autoradiographic mapping of M_3 muscarinic receptors in the rat brain. J. Pharmacol. Exp. Ther 264, 415–422. [PubMed: 8423541]

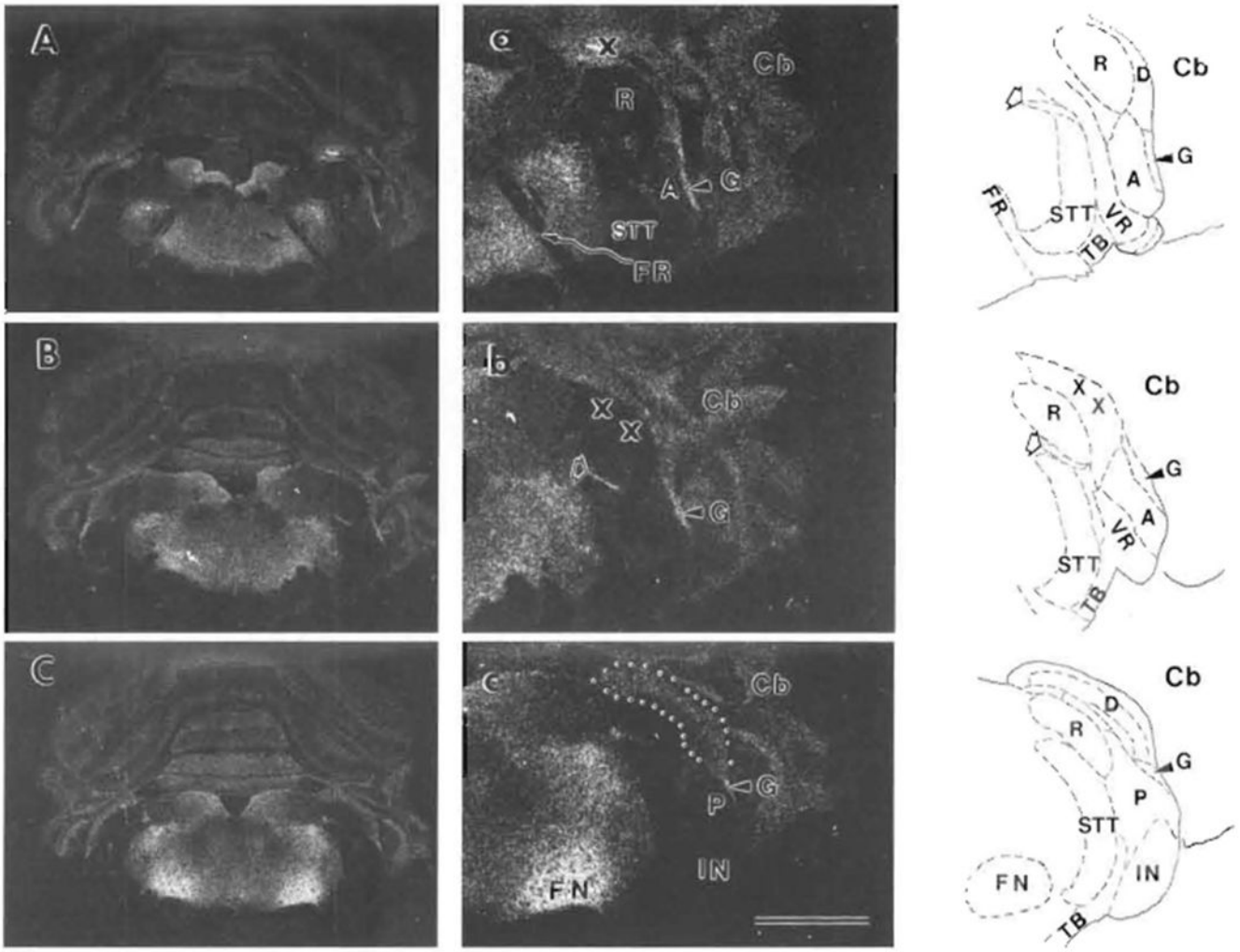

FIGURE 1. Autoradiographic images of [^{3}H]NMS binding sites in rat CN and nearly regions.

Tranverse sections through the lower brainstem are shown from more rostral (A) to more caudal (C). Higher magnification views of CN and nearby regions from the right sides of (A), (B) and (C) are shown in (a), (b) and (c). Tracings of the right sides of these same 3 sections after staining for AChE show regional boundaries: solid lines for outside boundaries and dashed lines for inside boundaries. The cerebellum (Cb) is lateral to the cochlear nucleus. The X symbol in (a) indicates a tissue fold. In (a) and (b) and their tracings, outlined arrow points to the location of the centrifugal labyrinthine bundle, which includes the olivocochlear bundle. The CN in (b) was damaged during processing, and the X symbols indicate position of lost DCN tissue. In (c), the DCN is outlined by dots. Both distances between sections are 150 μm. Abbreviations are identified in Table of Abbreviations. Also, AVCN is labeled by A, PVCN by P, DCN by D, granular region by G, and restiform body by R. Scale bar in (c) represents 3 mm for (A), (B) and (C), and 1.5 mm for (a), (b) and (c). Top is dorsal for all.

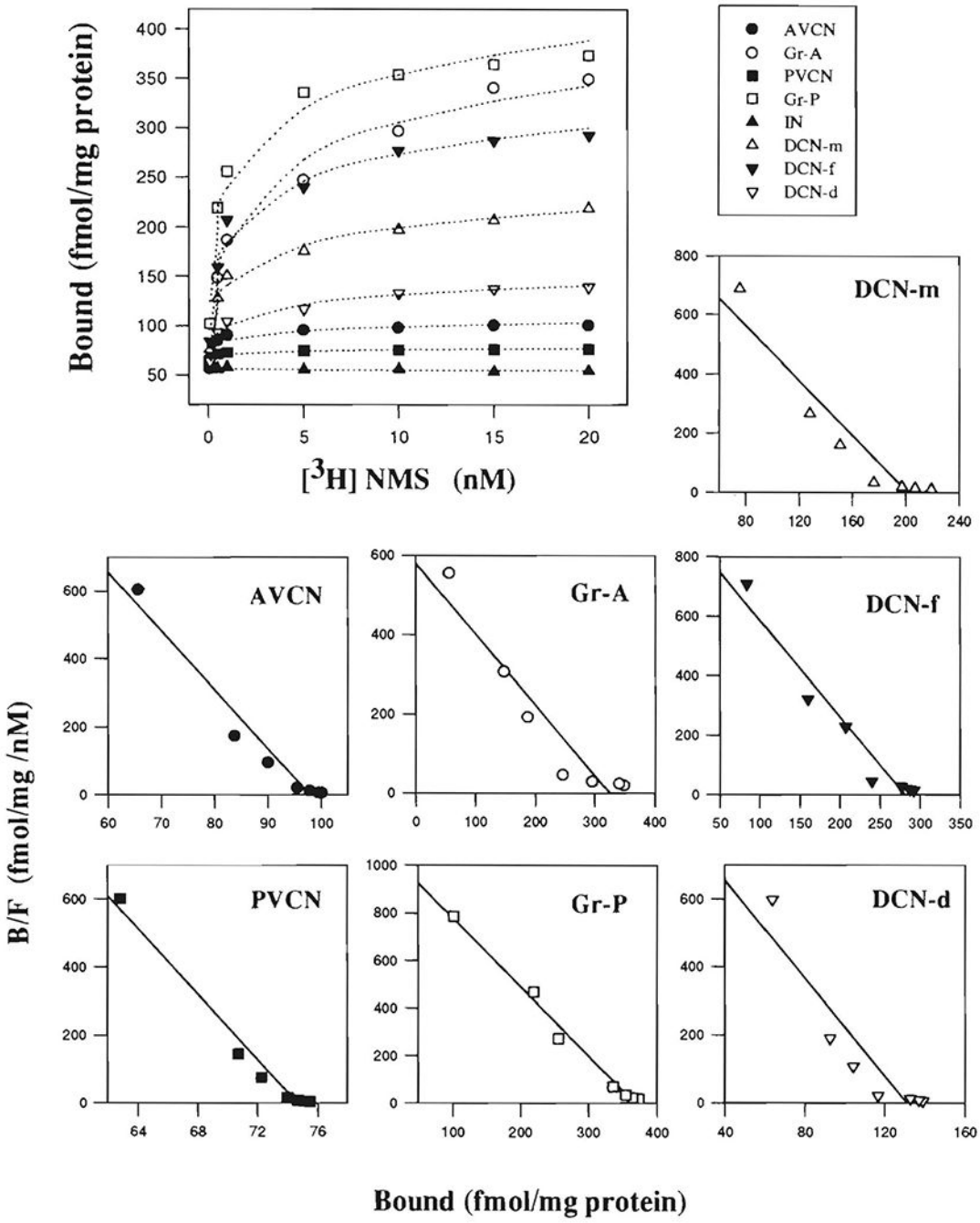

FIGURE 2. Autoradiographic determination of saturating [^{3}H]NMS binding to rat CN subregions.

Saturation curves are displayed in the large figure (top). Individual Rosenthall plots for subregions are displayed in the small figures to illustrate determination of K_d (−1/slope) and B_{max}. (*x* intercept) of NMS binding to them. Rosenthall plot is not shown for IN since measured density of NMS binding there was not significantly different from background. B/F indicates ratio of bound to free ligand concentrions. Abbreviations are identified in Table of Abbreviations.

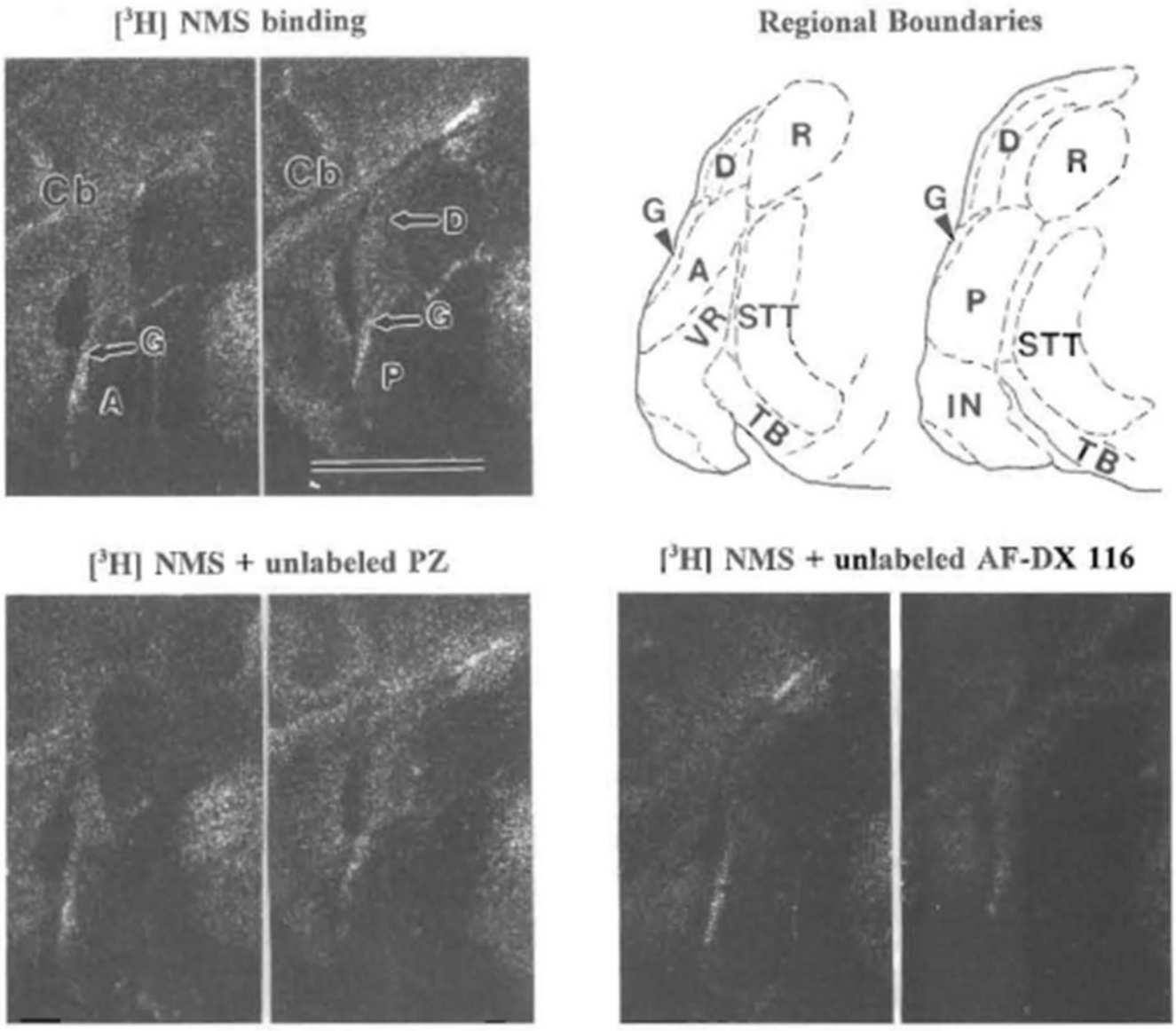

FIGURE 3. Autoradiograms of [^{3}H]NMS binding, and competitive binding with unlabeled subtype-preferential antagonists, to CN subregions.

Top left is 1 nM[^{3}H]NMS binding: left picture is more rostral showing AVCN (A); right picture is 225 μm more caudal, showing PVCN (P) and DCN (D); G indicates granular region. On top right, tracings of these two sections after staining with cresyl violet show regional boundaries: solid lines for outside boundaries and dashed lines for inside boundaries. Examples of inhibition of 1 nM [^{3}H]NMS binding by 100 nM of unlabeled PZ (sections 15 μm rostral to those in top row) and AF-DX 116 (30 μm caudal) are shown on bottom. Abbreviations are identified in Table of Abbreviations. Scale bar = 2 mm and applies to all autoradiograms. Top is dorsal and left is lateral for all.

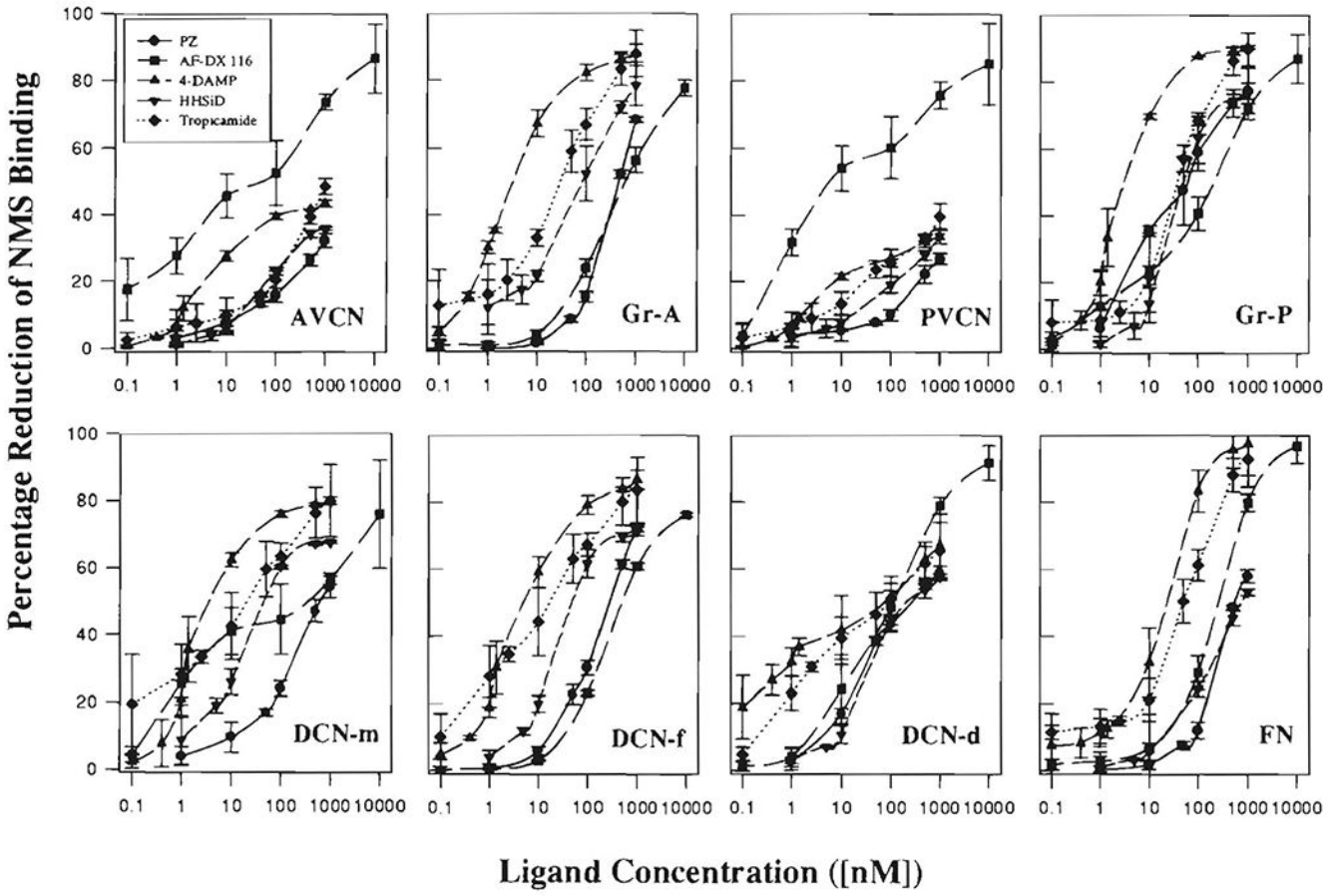

FIGURE 4. Inhibition of [^{3}H]NMS binding to rat CN subregions and FN by unlabeled PZ, AF-DX 116, 4-DAMP, HHSiD and tropicamide.

For each concentration of each unlabeled antagonist ligand, the binding density of 1 nM [^{3}H]NMS to each CN subregion (as shown in Fig. 3) was subtracted from the binding density of 1 nM [^{3}H]NMS in the absence of antagonist ($Density_{NMS} - Density_{NMS+antagonist}$) and then multiplied by 100 to generate the percentage inhibition. Means (± S.D.) of the results from three animals are shown.

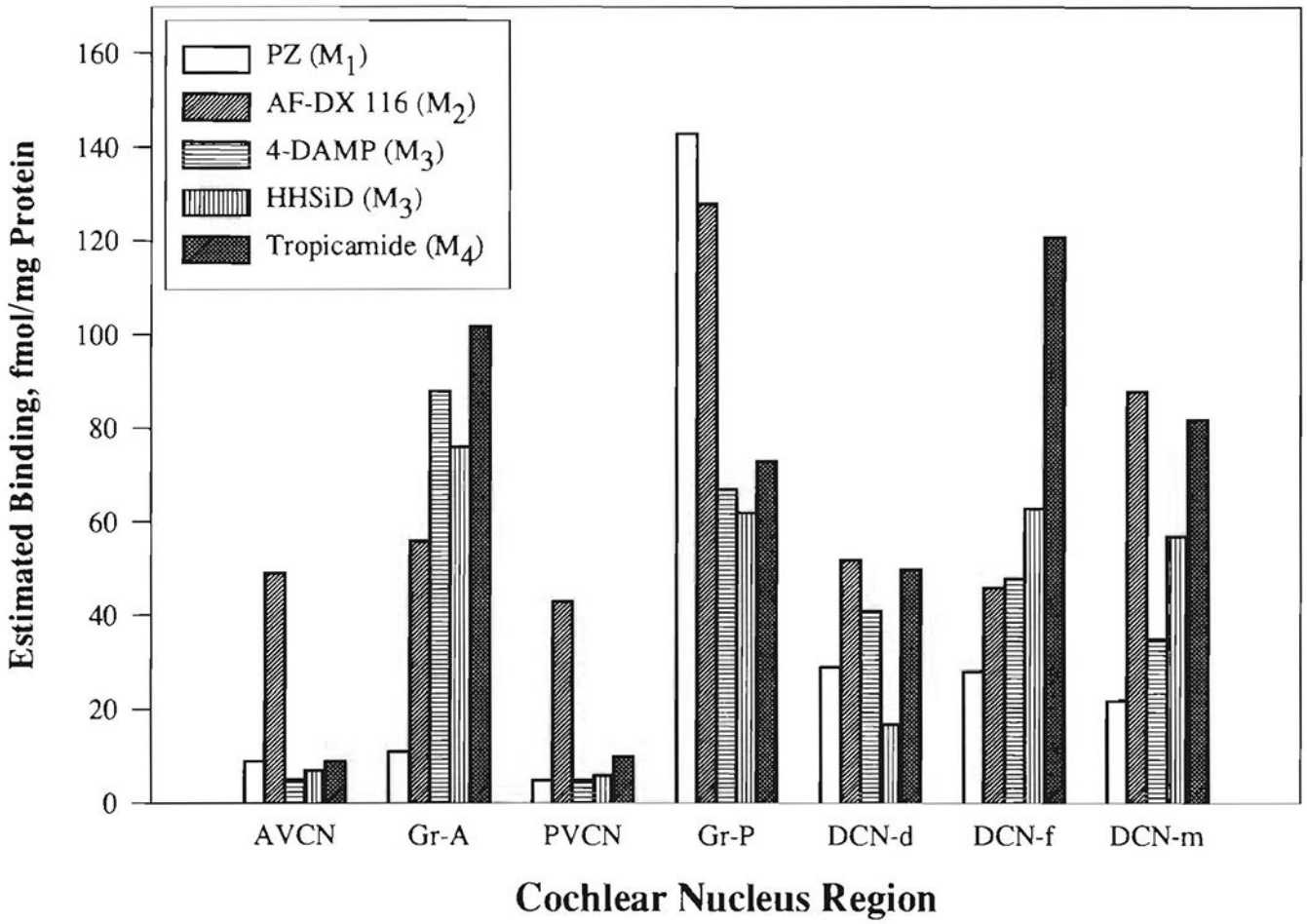

FIGURE 5. Estimated distributions of muscarinic receptor subtypes among rat cochlear nucleus regions.

Percentage displacement (%) of [^{3}H]NMS binding in each region by the ligand at a concentration equal to the mean high-affinity K_i for its preferred substrate (from Table II, average of K_is marked with *: PZ (M_1) = 14 nM; AF-DX 116 (M_2) = 40 nM; 4-DAMP (M_3) = 0.79 nM; HHSiD (M_3) = 12 nM; tropicamide (M_4) = 7.6 nM) was calculated (from Fig. 4) and multiplied by the total binding of [^{3}H]NMS for that region. Abbreviations are identified in Table of Abbreviations.

TABLE I

Autoradiographic saturation analysis of [^{3}H] NMS binding to rat cochlear nucleus and facial nucleus (mean ± S.E.M. for 3 rats)

Region	B_{max}(fmol/mg)	K_d (nM)	Hill Coefficient
AVCN	98.6 ± 6.1	0.06 ± 0.02	0.83 ± 0.19
Gr-A	331.1 ± 30.4	0.66 ± 0.27	0.68 ± 0.17
PVCN	75.1 ± 5.2	0.02 ± 0.02	0.56 ± 0.16
Gr-P	368.9 ± 40.7	0.34 ± 0.14	0.87 ± 0.21
DCN-d	131.1 ± 10.6	0.14 ± 0.06	0.50 ± 0.25
DCN-f	282.8 ± 19.9	0.32 ± 0.03	1.05 ± 0.28
DCN-m	202.3 ± 13.7	0.23 ± 0.11	0.77 ± 0.22
FN	1463.1 ± 64.2	1.78 ± 0.20	0.99 ± 0.30

TABLE II

Competitive binding of unlabeled ligands to cochlear nucleus regions and the facial nucleus[(1)].

	PZ (M_1)		AF-DX 116 (M_2)		4-DAMP (M_3)		HHSiD (M_3)		Tropicamide (M_4)	
	IC_{50}	K_i	IC_{50}	K_i	IC_{50}	K_i	IC_{50}	K_i	IC_{50}	K_i
AVCN	_[(2)]	–	43.9 ± 6.4	*2.5 ± 0.4	–	–	–	–	–	–
Gr-A	439.4 ± 3.7	174.7 ± 1.5	662.9 ± 96.0	263.6 ± 38.2	3.4 ± 0.1	1.4 ± 0.1	84.8 ± 8.3	33.7 ± 3.3	28.4 ± 3.7	*11.3 ± 1.5
PVCN	–	–	6.6 ± 5.8	*0.1 ± 0.1	–	–	–	–	–	–
Gr-P	56.2 ± 27.4	*14.3[(3)] ± 7.0	204.5 ± 118.9	*51.9 ± 30.2	3.3 ± 0.4	*0.8 ± 0.1	52.0 ± 19.3	*13.2 ± 4.9	34.3 ± 4.5	*8.7 ± 1.1
DCN-d	247.1 ± 13.3	30.3 ± 1.6	113.1 ± 20.6	*13.9 ± 2.5	64.7 ± 6.7	7.9 ± 0.8	275.0 ± 24.6	33.8 ± 3.0	84.8 ± 7.6	*10.4 ± 0.9
DCN-f	279.5 ± 21.7	67.8 ± 5.3	497.1 ± 39.4	*120.5 ± 9.5	5.2 ± 0.5	1.3 ± 0.1	51.8 ± 3.4	*12.6 ± 0.8	16.1 ± 1.8	*3.9 ± 0.4
DCN-m	631.0 ± 88.8	118.0 ± 16.6	284.2 ± 44.4	*53.1 ± 8.3	4.0 ± 1.3	*0.7 ± 0.2	49.7 ± 2.9	*9.3 ± 0.5	19.8 ± 2.4	*3.7 ± 0.4
FN	539.7 ± 78.7	345.6 ± 50.4	253.3 ± 35.4	*162.2 ± 22.7	22.8 ± 3.5	14.6 ± 2.3	749.9 ± 75.5	480.1 ± 48.3	47.7 ± 7.2	30.5 ± 4.6

[(1)] Values represent means ± S.E.M (nM) from three experiments (3 animals).

[(2)] In AVCN and PVCN, only AF-DX 116 demonstrated more than 50% inhibition of [^{3}H]NMS binding at the concentrations tested.

[(3)] Values marked with * are less than the mean + S.D. of K_i averaged from values in the literature (see Table III).

TABLE III

Mean K_i values, ± S.D., from the literature [(1)]

	M_1	M_2	M_3	M_4	M_5
PZ	13.8 ± 7.2	412.6 ± 240.9	276.3 ± 174.3	180.4 ± 206.4	268.0 ± 311.7
AF-DX 116	902.5 ± 469.1	104.6 ± 62.7	1146.6 ± 402.7	703.0 ± 707.6	2163.3 ± 650.4
4-DAMP	2.2 ± 1.5	9.3 ± 4.1	0.9 ± 0.2	2.1 ± 1.8	1.1 ± 0.1
HHSiD	24.7 ± 16.8	215.3 ± 29.2	12.4 ± 4.0	26.2 ± 13.9	52.9 ± 14.3
Tropicamide	53.7	45.7	50.1	15.1	

[(1)]References: Buckley et al., 1989; Ehlert et al., 1989; Lazareno et al., 1990; Waelbroeck et al., 1990; Dorje et al., 1991; Fernando et al., 1991; Frey and Howland, 1992; Kashihara et al., 1992; Lazareno and Birdsall, 1993; Zubieta and Frey, 1993.